

Thermal axion production in the primordial quark-gluon plasma

Peter Graf and Frank Daniel Steffen

Max-Planck-Institut für Physik, Föhringer Ring 6, D-80805 Munich, Germany

We calculate the rate for thermal production of axions via scattering of quarks and gluons in the primordial quark-gluon plasma. To obtain a finite result in a gauge-invariant way that is consistent to leading order in the strong gauge coupling, we use systematic field theoretical methods such as hard thermal loop resummation and the Braaten–Yuan prescription. The thermally produced yield, the decoupling temperature, and the density parameter are computed for axions with a mass below 10 meV. In this regime, with a Peccei–Quinn scale above 6×10^8 GeV, the associated axion population can still be relativistic today and can coexist with the axion cold dark matter condensate.

PACS numbers: 14.80.Va, 98.80.Cq, 95.35.+d, 95.30.Cq

I. INTRODUCTION

If the Peccei–Quinn (PQ) mechanism is the explanation of the strong CP problem, axions will pervade the Universe as an extremely weakly interacting light particle species. In fact, an axion condensate is still one of the most compelling explanations of the cold dark matter in our Universe [1, 2]. While such a condensate would form at temperatures $T \lesssim 1$ GeV, additional populations of axions can originate from processes at much higher temperatures. Even if the reheating temperature T_R after inflation is such that axions were never in thermal equilibrium with the primordial plasma, they can be produced efficiently via scattering of quarks and gluons. Here we calculate for the first time the associated thermal production rate consistent to leading order in the strong gauge coupling g_s in a gauge-invariant way. The result allows us to compute the associated relic abundance and to estimate the critical T_R value below which our considerations are relevant. For a higher value of T_R , one will face the case in which axions were in thermal equilibrium with the primordial plasma before decoupling at the temperature T_D as a hot thermal relic [1, 3]. The obtained critical T_R value can then be identified with the axion decoupling temperature T_D .

We focus on the model-independent axion (a) interactions with gluons given by the Lagrangian¹

$$\mathcal{L}_a = \frac{g_s^2}{32\pi^2 f_{\text{PQ}}} a G_{\mu\nu}^b \tilde{G}^{b\mu\nu}, \quad (1)$$

with the gluon field strength tensor $G_{\mu\nu}^b$, its dual $\tilde{G}_{\mu\nu}^b = \epsilon_{\mu\nu\rho\sigma} G^{b\rho\sigma}/2$, and the scale f_{PQ} at which the PQ symmetry is broken spontaneously. Numerous laboratory, astrophysical, and cosmological studies point to

$$f_{\text{PQ}} \gtrsim 6 \times 10^8 \text{ GeV}, \quad (2)$$

which implies that axions are stable on cosmological timescales [4, 5]. Considering this f_{PQ} range, we can neglect axion production via $\pi\pi \rightarrow \pi a$ in the primordial hot hadronic gas [6, 7]. Moreover, Primakoff processes such as $e^-\gamma \rightarrow e^- a$ or $q\gamma \rightarrow q a$ are not taken into account. These processes depend on the axion model and involve the electromagnetic coupling instead of the strong one such that they are usually far less efficient in the early Universe [8].

We assume a standard thermal history and refer to T_R as the initial temperature of the radiation-dominated epoch. While inflation models can point to T_R well above 10^{10} GeV, we focus on the case $T_R < f_{\text{PQ}}$ such that no PQ symmetry restoration takes place after inflation.

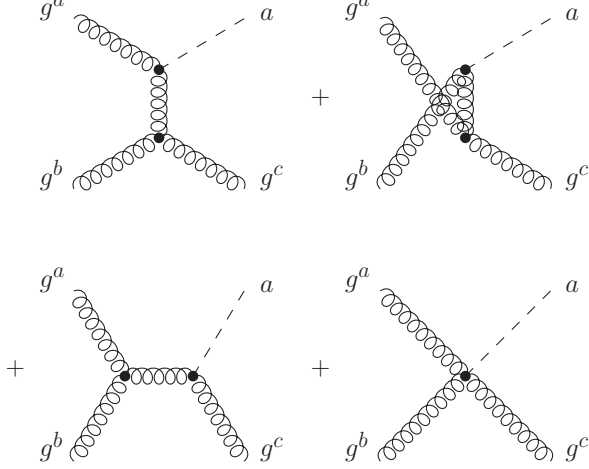
Related studies exist. The decoupling of axions out of thermal equilibrium with the primordial quark-gluon plasma (QGP) was considered in Refs. [1, 3]. While the same QCD processes are relevant, our study treats the thermal production of axions that were never in thermal equilibrium. Moreover, we use hard thermal loop (HTL) resummation [9] and the Braaten–Yuan prescription [10], which allow for a systematic gauge-invariant treatment of screening effects in the QGP. In fact, that prescription was introduced on the example of axion production in a hot QED plasma [10]; see also Ref. [11].

II. THERMAL PRODUCTION RATE

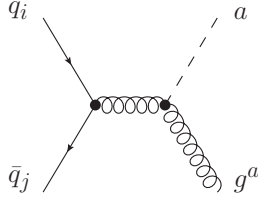
Let us calculate the thermal production rate of axions with energies $E \gtrsim T$ in the hot QGP. The relevant $2 \rightarrow 2$ scattering processes involving (1) are shown in Fig. 1. The corresponding squared matrix elements are listed in Table I, where $s = (P_1 + P_2)^2$ and $t = (P_1 - P_3)^2$ with P_1, P_2, P_3 , and P referring to the particles in the given order. Working in the limit $T \gg m_i$, the masses of all particles involved have been neglected. Sums over initial and final spins have been performed. For quarks, the contribution of a single chirality is given. The results obtained for processes A and C point to potential IR divergences associated with the exchange of soft (massless) gluons in the t channel and u channel. Here screening effects of the plasma become relevant. To account for

¹ The relation of f_{PQ} to the vacuum expectation value $\langle\phi\rangle$ that breaks the $U(1)_{\text{PQ}}$ symmetry depends on the axion model and the associated domain wall number N : $f_{\text{PQ}} \propto \langle\phi\rangle/N$; cf. [1, 2] and references therein.

Process A: $g^a + g^b \rightarrow g^c + a$



Process B: $q_i + \bar{q}_j \rightarrow g^a + a$



Process C: $q_i + g^a \rightarrow q_j + a$ (crossing of B)

FIG. 1. The 2 \rightarrow 2 processes for axion production in the QGP. Process C also exists with antiquarks $\bar{q}_{i,j}$ replacing $q_{i,j}$.

such effects, the QCD Debye mass $m_D = \sqrt{3}m_g$, with $m_g = g_s T \sqrt{N_c + (n_f/2)}/3$ for $N_c = 3$ colors and $n_f = 6$ flavors, was used in Ref. [3]. In contrast, our calculation relies on HTL resummation [9, 10] which treats screening effects more systematically.

Following Ref. [10], we introduce a momentum scale k_{cut} such that $g_s T \ll k_{\text{cut}} \ll T$ in the weak coupling limit $g_s \ll 1$. This separates soft gluons with momentum transfer of order $g_s T$ from hard gluons with momentum transfer of order T . By summing the respective soft and

hard contributions, the finite rate for thermal production of axions with $E \gtrsim T$ is obtained in leading order in g_s ,

$$E \frac{dW_a}{d^3p} = E \frac{dW_a}{d^3p} \Big|_{\text{soft}} + E \frac{dW_a}{d^3p} \Big|_{\text{hard}}, \quad (3)$$

which is independent of k_{cut} ; cf. (5) and (7) given below.

In the region with $k < k_{\text{cut}}$, we obtain the soft contribution from the imaginary part of the thermal axion self-energy with the ultraviolet cutoff k_{cut} ,

$$E \frac{dW_a}{d^3p} \Big|_{\text{soft}} = -\frac{f_B(E)}{(2\pi)^3} \text{Im} \Pi_a(E + i\epsilon, \vec{p}) \Big|_{k < k_{\text{cut}}} \quad (4)$$

$$= E f_B(E) \frac{3m_g^2 g_s^4 (N_c^2 - 1) T}{8192 \pi^8 f_{\text{PQ}}^2} \left[\ln \left(\frac{k_{\text{cut}}^2}{m_g^2} \right) - 1.379 \right] \quad (5)$$

with the equilibrium phase space density for bosons (fermions) $f_{\text{B(F)}}(E) = [\exp(E/T) \mp 1]^{-1}$. Our derivation of (5) follows Ref. [10]. The leading order contribution to $\text{Im} \Pi_a$ for $k < k_{\text{cut}}$ and $E \gtrsim T$ comes from the Feynman diagram shown in Fig. 2. Because of $E \gtrsim T$, only one of the two gluons can have a soft momentum. Thus only one effective HTL-resummed gluon propagator is needed.

In the region with $k > k_{\text{cut}}$, bare gluon propagators can be used since k_{cut} provides an IR cutoff. From the results given in Table I weighted with appropriate multiplicities, statistical factors, and phase space densities, we then obtain the (angle-averaged) hard contribution

$$E \frac{dW_a}{d^3p} \Big|_{\text{hard}} = \frac{1}{2(2\pi)^3} \int \frac{d\Omega_p}{4\pi} \int \left[\prod_{j=1}^3 \frac{d^3 p_j}{(2\pi)^3 2E_j} \right] \times (2\pi)^4 \delta^4(P_1 + P_2 - P_3 - P) \Theta(k - k_{\text{cut}}) \times \sum f_1(E_1) f_2(E_2) [1 \pm f_3(E_3)] |M_{1+2 \rightarrow 3+a}|^2 \quad (6)$$

$$= E \frac{g_s^6 (N_c^2 - 1)}{512 \pi^7 f_{\text{PQ}}^2} \left\{ n_f \frac{f_B(E) T^3}{48\pi} \ln(2) + \left(N_c + \frac{n_f}{2} \right) \frac{f_B(E) T^3}{48\pi} \left[\ln \left(\frac{T^2}{k_{\text{cut}}^2} \right) + \frac{17}{3} - 2\gamma + \frac{2\zeta'(2)}{\zeta(2)} \right] + N_c (I_{\text{BBB}}^{(1)} - I_{\text{BBB}}^{(3)}) + n_f (I_{\text{FBF}}^{(1)} + I_{\text{FFB}}^{(3)}) \right\} \quad (7)$$

TABLE I. Squared matrix elements for axion (a) production in 2-body processes involving quarks of a single chirality (q_i) and gluons (g^a) in the high-temperature limit, $T \gg m_i$, with the $\text{SU}(N_c)$ color matrices f^{abc} and T_{ji}^a . Sums over initial and final state spins have been performed.

| Label i | Process i | $ M_i ^2 / \left(\frac{g_s^6}{128 \pi^4 f_{\text{PQ}}^2} \right)$ |
|-----------|---------------------------------------|--|
| A | $g^a + g^b \rightarrow g^c + a$ | $-4 \frac{(s^2 + st + t^2)^2}{st(s+t)} f^{abc} ^2$ |
| B | $q_i + \bar{q}_j \rightarrow g^a + a$ | $\left(\frac{2t^2}{s} + 2t + s \right) T_{ji}^a ^2$ |
| C | $q_i + g^a \rightarrow q_j + a$ | $\left(-\frac{2s^2}{t} - 2s - t \right) T_{ji}^a ^2$ |

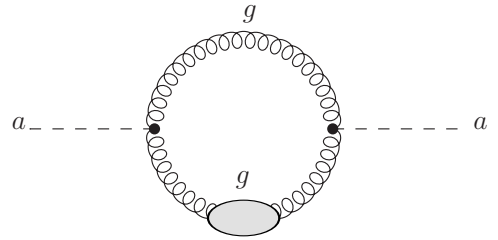


FIG. 2. Leading contribution to the axion self-energy for soft gluon momentum transfer and hard axion energy. The blob on the gluon line denotes the HTL-resummed gluon propagator.

with Euler's constant γ , Riemann's zeta function $\zeta(z)$,

$$I_{\text{BBB(FBF)}}^{(1)} = \frac{1}{32\pi^3} \int_0^\infty dE_3 \int_0^{E+E_3} dE_1 \ln \left(\frac{|E_1 - E_3|}{E_3} \right) \\ \times \left\{ -\Theta(E_1 - E_3) \frac{d}{dE_1} \left[f_{\text{BBB(FBF)}} \frac{E_2^2}{E^2} (E_1^2 + E_3^2) \right] \right. \\ \left. + \Theta(E_3 - E_1) \frac{d}{dE_1} [f_{\text{BBB(FBF)}} (E_1^2 + E_3^2)] \right. \\ \left. + \Theta(E - E_1) \frac{d}{dE_1} \left[f_{\text{BBB(FBF)}} \left(\frac{E_1^2 E_2^2}{E^2} - E_3^2 \right) \right] \right\}, \quad (8)$$

$$I_{\text{BBB(FFB)}}^{(3)} = \frac{1}{32\pi^3} \int_0^\infty dE_3 \int_0^{E+E_3} dE_2 f_{\text{BBB(FFB)}} \\ \times \left\{ \Theta(E - E_3) \frac{E_1^2 E_3^2}{E^2 (E_3 + E)} + \Theta(E_3 - E) \frac{E_2^2}{E_3 + E} \right. \\ \left. + [\Theta(E_3 - E)\Theta(E_2 - E_3) - \Theta(E - E_3)\Theta(E_3 - E_2)] \right. \\ \left. \times \frac{E_2 - E_3}{E^2} [E_2(E_3 - E) - E_3(E_3 + E)] \right\}, \quad (9)$$

$$f_{\text{BBB,FBF,FFB}} = f_1(E_1)f_2(E_2)[1 \pm f_3(E_3)]. \quad (10)$$

The sum in (6) is over all axion production processes $1 + 2 \rightarrow 3 + a$ viable with (1). The colored particles 1–3 were in thermal equilibrium at the relevant times. Performing the calculation in the rest frame of the plasma, f_i are thus described by $f_{\text{F/B}}$ depending on the respective spins. Shorthand notation (10) indicates the corresponding combinations, where $+$ ($-$) accounts for Bose enhancement (Pauli blocking) when particle 3 is a boson (fermion). With any initial axion population diluted away by inflation and T well below T_{D} so that axions are not in thermal equilibrium, the axion phase space density f_a is negligible in comparison to $f_{\text{F/B}}$. Thereby, axion disappearance reactions ($\propto f_a$) are neglected as well as the respective Bose enhancement ($1 + f_a \approx 1$). Details on the methods applied to obtain our results (7)–(9) can be found in Refs. [11–13].

III. RELIC AXION ABUNDANCE

We now calculate the thermally produced (TP) axion yield $Y_a^{\text{TP}} = n_a/s$, where n_a is the corresponding axion number density and s the entropy density. For T sufficiently below T_{D} , the evolution of the thermally produced n_a with cosmic time t is governed by the Boltzmann equation

$$\frac{dn_a}{dt} + 3Hn_a = \int d^3p \frac{dW_a}{d^3p} = W_a. \quad (11)$$

Here H is the Hubble expansion rate, and the collision term is the integrated thermal production rate

$$W_a = \frac{\zeta(3)g_s^6 T^6}{64\pi^7 f_{\text{PQ}}^2} \left[\ln \left(\frac{T^2}{m_g^2} \right) + 0.406 \right]. \quad (12)$$

Assuming conservation of entropy per comoving volume element, (11) can be written as $dY_a^{\text{TP}}/dt = W_a/s$. Since thermal axion production proceeds basically during the hot radiation-dominated epoch, i.e., well above the temperature of radiation-matter equality $T_{\text{mat=rad}}$, one can change variables from cosmic time t to temperature T accordingly. With initial temperature T_{R} at which $Y_a^{\text{TP}}(T_{\text{R}}) = 0$, the relic axion yield today is given by

$$Y_a^{\text{TP}} \approx Y_a^{\text{TP}}(T_{\text{mat=rad}}) = \int_{T_{\text{mat=rad}}}^{T_{\text{R}}} dT \frac{W_a(T)}{Ts(T)H(T)} \\ = 18.6g_s^6 \ln \left(\frac{1.501}{g_s} \right) \left(\frac{10^{10} \text{ GeV}}{f_{\text{PQ}}} \right)^2 \left(\frac{T_{\text{R}}}{10^{10} \text{ GeV}} \right). \quad (13)$$

This result is shown by the diagonal lines in Fig. 3 for cosmological scenarios with different T_{R} values ranging from 10^4 to 10^{12} GeV. Here we use $g_s = g_s(T_{\text{R}})$ as described by the 1-loop renormalization group evolution [5]

$$g_s(T_{\text{R}}) = \left[g_s^{-2}(M_Z) + \frac{11N_c - 2n_f}{24\pi^2} \ln \left(\frac{T_{\text{R}}}{M_Z} \right) \right]^{-1/2} \quad (14)$$

where $g_s^2(M_Z)/(4\pi) = 0.1172$ at $M_Z = 91.188$ GeV. Since the methods [9, 10] allowing for the gauge-invariant derivation require $g_s \ll 1$, (13) is most reliable for $T_{\text{R}} \gg 10^4$ GeV. If g_s is too large, unphysical negative values of (3) are encountered for $E \lesssim T$ that lead to an artificial suppression of (13) as indicated by the logarithmic factor; cf. Sec. 3 in Ref. [14] where a similar behavior

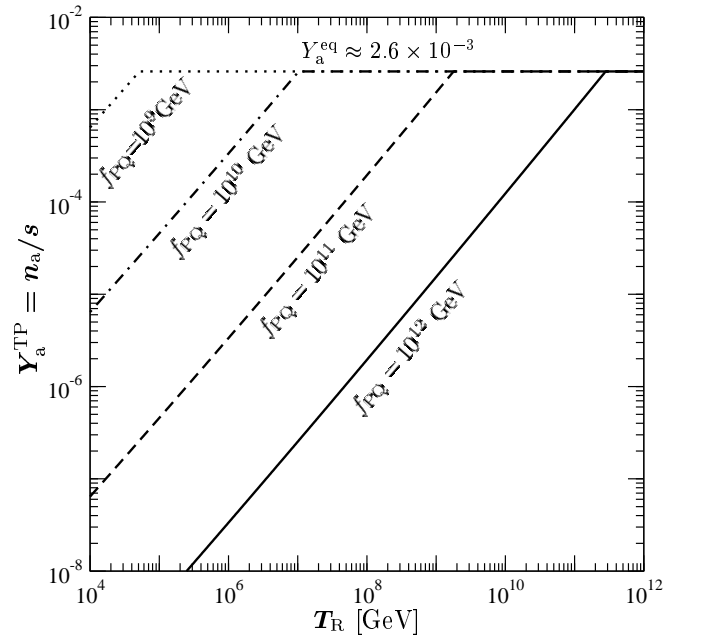


FIG. 3. The relic axion yield today originating from thermal processes in the primordial plasma for cosmological scenarios characterized by different T_{R} values covering the range from 10^4 to 10^{12} GeV. The dotted, dash-dotted, dashed, and solid lines are obtained for $f_{\text{PQ}} = 10^9, 10^{10}, 10^{11}$, and 10^{12} GeV.

is discussed in more detail. Nevertheless, we think that the applied methods still allow presently for the most reliable treatment since they respect gauge invariance.

Note that (13) is only valid when axion disappearance processes can be neglected. In scenarios in which T_R exceeds T_D , this is not justified since there has been an early period in which axions were in thermal equilibrium. In this period, their production and annihilation proceeded at equal rates. Thereafter, they decoupled as hot thermal relics at T_D , where all standard model particles are effectively massless. The present yield of those thermal relic axions is then given by $Y_a^{\text{eq}} = n_a^{\text{eq}}/s \approx 2.6 \times 10^{-3}$. In Fig. 3 this value is indicated by the horizontal lines. In fact, the thermally produced yield cannot exceed Y_a^{eq} . In scenarios with T_R such that (13) turns out to be close to or greater than Y_a^{eq} , disappearance processes have to be taken into account. The resulting axion yield from thermal processes will then respect Y_a^{eq} as the upper limit. For example, for $f_{\text{PQ}} = 10^9 \text{ GeV}$, this yield would show a dependence on the reheating temperature T_R that is very similar to the one shown by the dotted line in Fig. 3. The only difference will be a smooth transition instead of the kink at $Y_a^{\text{TP}} = Y_a^{\text{eq}}$.

IV. AXION DECOUPLING TEMPERATURE

The kinks in Fig. 3 indicate the critical T_R value which separates scenarios with thermal relic axions from those in which axions have never been in thermal equilibrium. Thus, for a given f_{PQ} , this critical T_R value allows us to extract an estimate of the axion decoupling temperature T_D . We find that our numerical results are well described by

$$T_D \approx 9.6 \times 10^6 \text{ GeV} \left(\frac{f_{\text{PQ}}}{10^{10} \text{ GeV}} \right)^{2.246}. \quad (15)$$

In a previous study [3], the decoupling of axions that were in thermal equilibrium in the QGP was calculated. When following [3] but including (14), we find that the temperature at which the axion yield from thermal processes started to differ by more than 5% from Y_a^{eq} agrees basically with (15). The axion interaction rate Γ equals H already at temperatures about a factor 4 below (15) which, however, amounts to a different definition of T_D .

V. AXION DENSITY PARAMETER

Since thermally produced axions have basically a thermal spectrum also, we find that the density parameter from thermal processes in the primordial plasma can be described approximately by

$$\Omega_a^{\text{TP/eq}} h^2 \simeq \sqrt{\langle p_{a,0} \rangle^2 + m_a^2} Y_a^{\text{TP/eq}} s(T_0) h^2 / \rho_c \quad (16)$$

with the present average momentum $\langle p_{a,0} \rangle = 2.701 T_{a,0}$ given by the present axion temperature $T_{a,0} = 0.332 T_0 \simeq$

0.08 meV , where $T_0 \simeq 0.235 \text{ meV}$ is the present cosmic microwave background temperature, $h \simeq 0.7$ is Hubble's constant in units of 100 km/Mpc/s and $\rho_c/[s(T_0)h^2] = 3.6 \text{ eV}$. A comparison of $T_{a,0}$ with the axion mass $m_a \simeq 0.6 \text{ meV} (10^{10} \text{ GeV}/f_{\text{PQ}})$ shows that this axion population is still relativistic today for $f_{\text{PQ}} \gtrsim 10^{11} \text{ GeV}$.

In Fig. 4 the solid, dashed, and dash-dotted lines show $\Omega_a^{\text{TP/eq}} h^2$ for $T_R = 10^6, 10^7$, and 10^8 GeV , respectively. In the f_{PQ} region to the right (left) of the respective kink, in which $T_R < T_D$ ($T_R > T_D$) holds, $\Omega_a^{\text{TP/eq}} h^2$ applies, which behaves as $\propto f_{\text{PQ}}^{-3}$ (f_{PQ}^{-1}) for $m_a \gg T_{a,0}$ and as $\propto f_{\text{PQ}}^{-2}$ (f_{PQ}^0) for $m_a \ll T_{a,0}$. The gray dotted curve shows $\Omega_a^{\text{eq}} h^2$ for higher T_R with $T_R > T_D$ and also indicates an upper limit on the thermally produced axion density. Observation of those axions will be extremely challenging. Even $\Omega_a^{\text{eq}} h^2$ stays well below the cold dark matter density $\Omega_{\text{CDM}} h^2 \simeq 0.1$ (gray horizontal bar) and also below the photon density $\Omega_\gamma h^2 \simeq 2.5 \times 10^{-5}$ (gray thin line) [5] in the allowed f_{PQ} range (2). There, the current hot dark matter limits are also safely respected [15].

In cosmological settings with $T_R > T_D$, axions produced nonthermally before axion decoupling (e.g., in inflaton decays) will also be thermalized resulting in $\Omega_a^{\text{eq}} h^2$. The axion condensate from the misalignment mechanism, however, is not affected—independent of the hierarchy between T_R and T_D —since thermal axion production in the QGP is negligible at $T \lesssim 1 \text{ GeV}$. Thus, the asso-

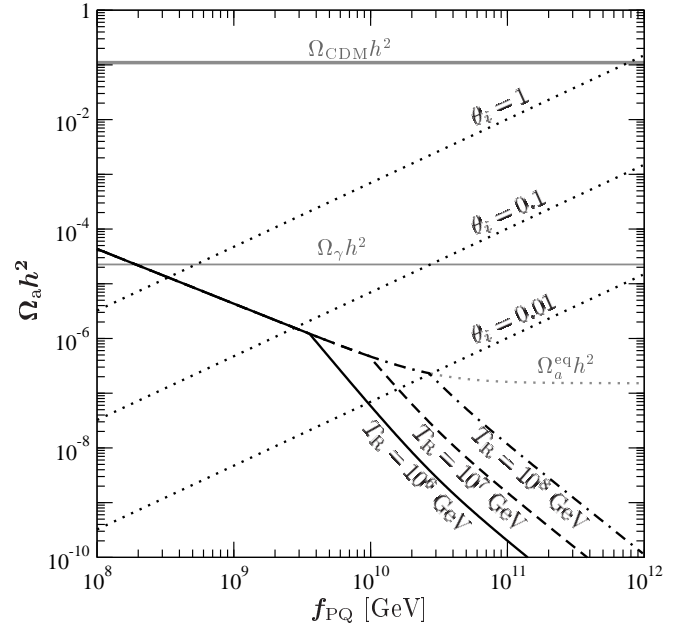


FIG. 4. The axion density parameter from thermal processes for $T_R = 10^6 \text{ GeV}$ (solid), 10^7 GeV (dashed) and 10^8 GeV (dash-dotted) and the one from the misalignment mechanism for $\theta_i = 1, 0.1$, and 0.01 (dotted). The density parameters for thermal relic axions, photons, and cold dark matter are indicated, respectively, by the gray dotted line ($\Omega_a^{\text{eq}} h^2$), the gray thin line ($\Omega_\gamma h^2$), and the gray horizontal bar ($\Omega_{\text{CDM}} h^2$).

ciated density $\Omega_a^{\text{MIS}} h^2 \sim 0.15 \theta_i^2 (f_{\text{PQ}}/10^{12} \text{ GeV})^{7/6}$ [1, 2, 16] can coexist with $\Omega_a^{\text{TP/eq}} h^2$ and is governed by the misalignment angle θ_i as illustrated by the dotted lines in Fig. 4. Thereby, the combination of the axion cold dark matter condensate with the axions from thermal processes, $\Omega_a h^2 = \Omega_a^{\text{MIS}} h^2 + \Omega_a^{\text{TP/eq}} h^2$, gives the analog of a Lee–Weinberg curve. Taking into account the relation between f_{PQ} and m_a , this is exactly the type of curve that can be inferred from Fig. 4. Here our calculation of thermal axion production in the quark-gluon

plasma allows us to cover, for the first time, also cosmological settings with $T_{\text{R}} < T_{\text{D}}$.

ACKNOWLEDGMENTS

We are grateful to Thomas Hahn, Josef Pradler, Georg Raffelt, and Javier Redondo for valuable discussions. This research was partially supported by the Cluster of Excellence “Origin and Structure of the Universe.”

-
- [1] P. Sikivie, Lect. Notes Phys. **741**, 19 (2008)
 - [2] J.E. Kim, G. Carosi, Rev. Mod. Phys. **82**, 557 (2008)
 - [3] E. Masso, F. Rota, G. Zsembinski, Phys. Rev. **D66**, 023004 (2002)
 - [4] G.G. Raffelt, Lect. Notes Phys. **741**, 51 (2008)
 - [5] C. Amsler et al. (PDG), Phys. Lett. **B667**, 1 (2008)
 - [6] S. Chang, K. Choi, Phys. Lett. **B316**, 51 (1993)
 - [7] S. Hannestad, A. Mirizzi, G. Raffelt, JCAP **0507**, 002 (2005)
 - [8] M.S. Turner, Phys. Rev. Lett. **59**, 2489 (1987)
 - [9] E. Braaten, R.D. Pisarski, Nucl. Phys. **B337**, 569 (1990)
 - [10] E. Braaten, T.C. Yuan, Phys. Rev. Lett. **66**, 2183 (1991)
 - [11] M. Bolz, A. Brandenburg, W. Buchmüller, Nucl. Phys. **B606**, 518 (2001); *ibid.* **B790** 336 (2008)
 - [12] J. Pradler, Electroweak Contributions to Thermal Gravitino Production, Diploma Thesis, Univ. of Vienna, 2006
 - [13] P. Graf, Axions in the Early Universe, Diploma Thesis, Univ. of Regensburg, 2009
 - [14] A. Brandenburg, F. D. Steffen, JCAP **0408** 008 (2004)
 - [15] S. Hannestad, A. Mirizzi, G.G. Raffelt, Y.Y.Y. Wong, JCAP **1008**, 001 (2010)
 - [16] M. Beltran, J. Garcia-Bellido and J. Lesgourgues, Phys. Rev. D **75**, 103507 (2007)